Observations and Models of the Debris Disk around the K Dwarf HD 92945

David Golimowski (JHU), John Krist (JPL), Christine Chen (NOAO), Karl Stapelfeldt (JPL), David Ardila (IPAC/SSC), Mark Clampin (GSFC), Glenn Schneider, Murray Silverstone (Arizona), Holland Ford (JHU), and Garth Illingworth (UCSC)

1. Introduction

A circumstellar disk is a "debris disk" if the age of its host star exceeds the lifetimes of the dust grains. The dust is replenished by collisions of planetesimals and/or cometary evaporation. Resolved images of debris disks enable studies of dust dynamics and composition and provide opportunities to indirectly detect planets via their dynamical effects on the dust.

Debris disks have small optical depths ($\tau \sim 10^{-3}$) and surround bright stars, so detection in scattered light is difficult without a coronagraph. Of the 11 debris disks resolved coronagraphically in scattered light, only 2 surround stars with masses $< 1\ M_\odot$: HD 53145 (K1V; Kalas et al. 2006) and AU Mic (M1Ve; Kalas et al. 2004). The dependencies of disk properties on stellar mass and age are undetermined, especially for low-mass stars ⇒ more examples needed.

HD 92945 is a ~100 Myr-old, nearby (~22 pc), bright (V =7.76) K1V star around which *IRAS* and *Spitzer* detected excess IR emission consistent with the presence of cold (~40 K) circumstellar dust (Silverstone 2000; Chen et al. 2005).

2. *Spitzer* Observations of HD 92945

❖ IRAC 3.6, 4.5, 5.8, 8.0 μm and MIPS 24 and 70 μm photometry obtained in 2004 as part of a *Spitzer* GTO search for debris disks around 69 young, nearby stars.

❖ Very-low-resolution (R~20) spectrum from 55-96 μm obtained in 2005 with MIPS SED mode under Program 241.

❖ Low-resolution (R~100) spectra obtained in 2005 with IRS Short-Low (5.2–14.5 μm) and Long-Low (14.0–35.4 μm) modes under Program 241.

❖ IRAC and MIPS 24 μm photometry is consistent with photospheric flux from a K1V star, but MIPS 70 μm flux is 60× larger than predicted stellar flux (Chen et al. 2005).

❖ Fractional dust luminosity ($L_{IR}/L_* = \tau \sim 7.7\times10^{-4}$) is about half that of the disk around β Pictoris.

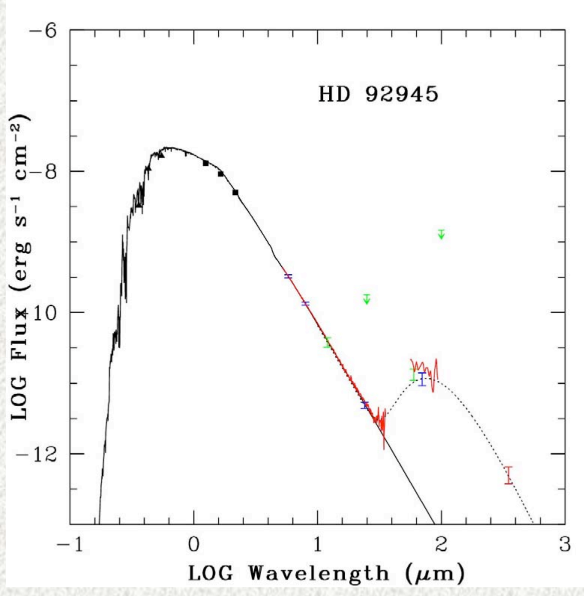

Fig. 1. *SED based on photometry from 2MASS (black squares), IRAS (green bars), Spitzer IRAC and MIPS (blue bars), and CSO SHARC-II 350 μm (red bar), and low-res IRS and MIPS spectra (red curves). The photosphere is fitted with a 1993 Kurucz model; the IR-excess is fitted with a modified blackbody with Teff=40 K and emissivity ∝ $\lambda^{-0.8}$. (Adapted from Chen et al. 2005.)*

3. *HST* Coronagraphic Imaging of the Disk

❖ ACS/HRC coronagraphic images of HD 92945 were obtained in Dec 2004 using the F606W (Broad V) filter and the d=1″.8 occulting spot. The exposures totalled 2200 s. The ACS observations are a collaborative effort between ACS and MIPS GTO teams.

❖ After detecting the disk, follow-up ACS images were obtained in July 2005 using the F606W and F814W (Broad I) filters and total exposures of 4870 s and 7600 s, respectively. The FOV was rolled 157° from its initial orientation.

❖ Similar images of the K0V star HD 100623 were recorded at each epoch for use as coronagraphic-PSF reference images.

❖ NICMOS coronagraphic images of HD 92945 were obtained in April 2005 using the F110W (J) filter. Two sets of 672 s exposures with a roll offset of 30° showed no evidence of the disk above the level of the PSF-subtraction residuals.

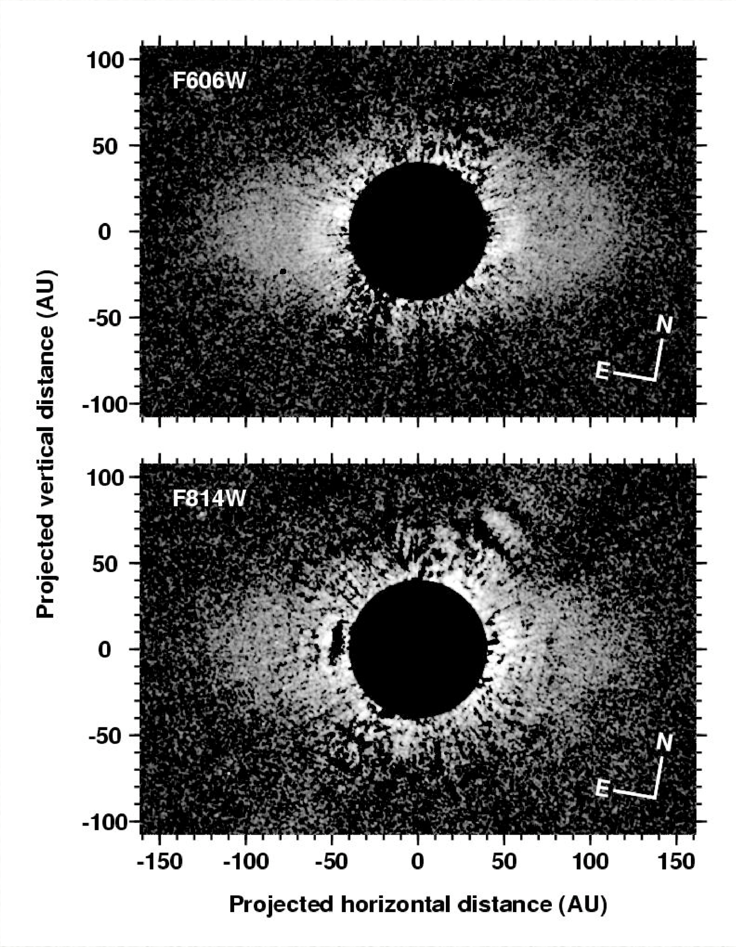

Fig. 2. *HRC images of the HD 92945 disk after subtraction of the PSF-reference star images. The images have been median filtered and corrected for geometric distortion. We exploited the roll offset between epochs to remove subtraction artifacts from the F606W image. A 2″ spot has been superposed to mask the central subtraction residuals.*

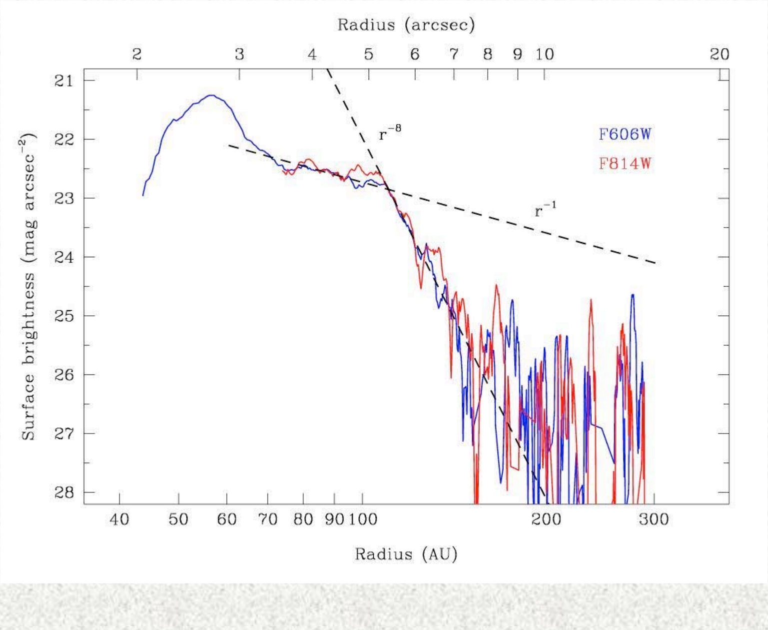

Fig. 3. *Radial surface brightness profiles along the major axis of the disk, after smoothing with an 11-pixel boxcar. The blue and red curves show the average F606W and F814W profiles of the east and west extensions of the disk, respectively. Power-law fits to the F606W profile from 3″.0–5″.1 and from 5″.1–6″.7 are overplotted as black dashed lines.* ***This plot shows that the disk is colorless and effectively truncated beyond 5″.1 (110 AU).***

4. Mapping the Column Density of the Dust

❖ The disk appears inclined to the line of sight by ~29° and exhibits a relatively bright ring of radius ~2″.6 (~57 AU) and thickness ~0″.7 (~16 AU).

❖ The lack of azimuthal brightness asymmetry suggests the dust scatters mostly isotropically.

❖ We deprojected the F606W image to appear "face on," and scaled the image by r^2 to compensate for the inverse-square illumination from the star.

❖ Assuming uniform dust albedo, the deprojected and scaled image is a proxy for a map of the vertical column density of the dust.

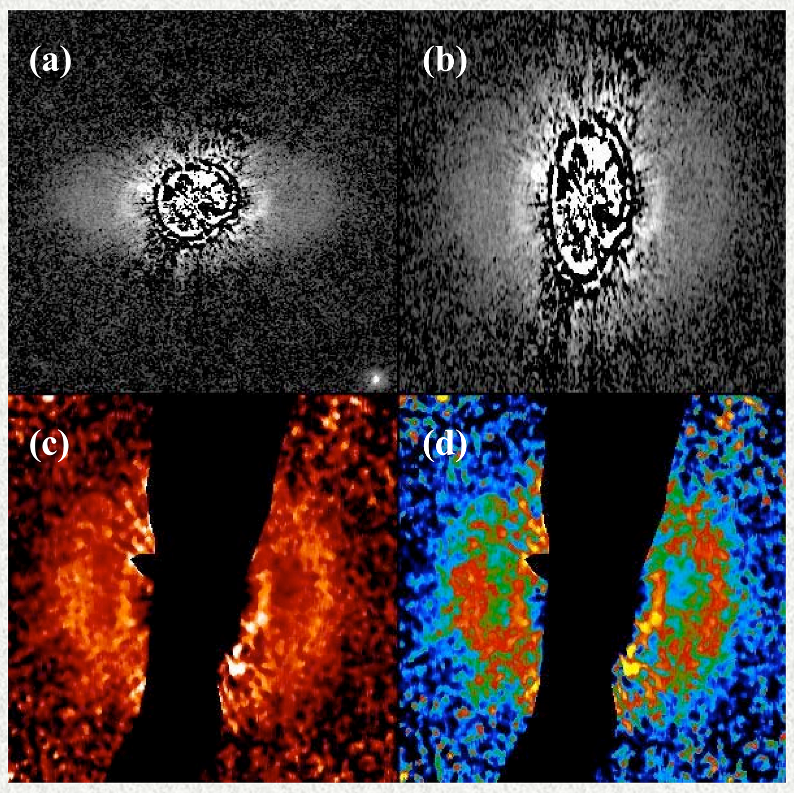

Fig. 4. *(a) Same F606W image as in Fig. 2, but without the software mask; (b) deprojected F606W image, assuming a circular disk with inclination of 29°; (c) and (d) false-color deprojected images after scaling by r^2 to compensate for the inverse-square illumination from the star. Subtraction residuals have been masked. Note the brightness (density) enhancements at the inner and outer edges of the disk.*

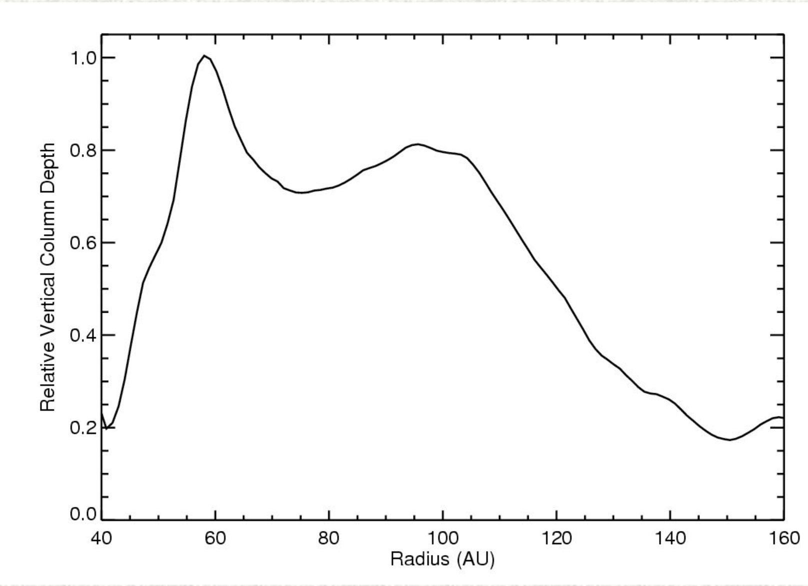

Fig. 5. *Radial profile of the relative column density of the dust, obtained by azimuthally averaging the density maps shown in Figs. 4(c) and (d).*

5. Scattered-Light Model of the Disk

❖ We fitted a multizonal, 3-D scattering model (2-D spatial + 1-D scattering) to our F606W image of the HD 92945 disk using the code previously used to model the edge-on debris disk around AU Mic (Krist et al. 2005).

❖ The annular zones and their respective radial density profiles were defined by a series of 7 contiguous power-law approximations to the radial density profile shown in Fig. 5.

❖ The inclination of the disk prevents constraint of the disk flaring angle, so we assumed a flat disk with a Lorentzian vertical profile and a FWHM of 4 AU.

❖ A Henyey-Greenstein scattering phase function was included in the model.

❖ The resulting best-fit model indicates isotropic scattering (g = 0) and an inclination of 28.6°.

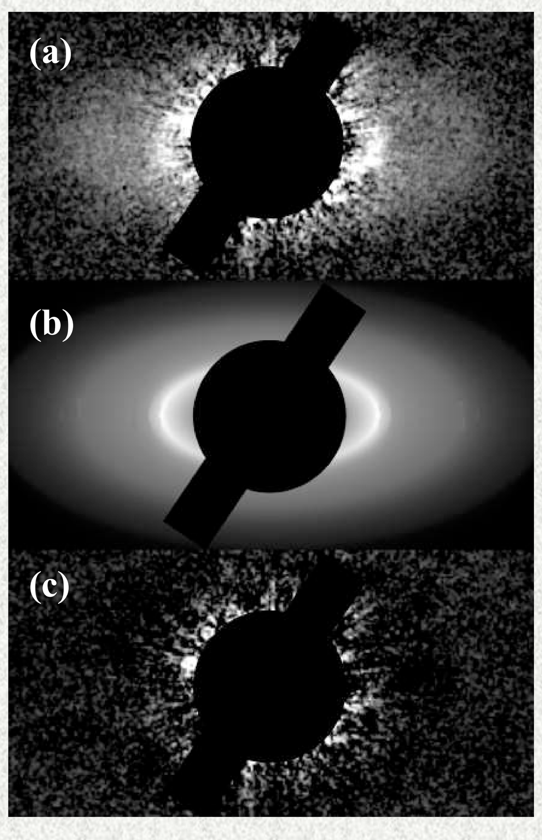

Fig. 6. *Scattered-light model of the disk. (a) F606W image overlaid with residual mask. (b) Best-fit 7 zone model to the F606W image. (c) Residual image of after subtraction of the model (b) from image (a).*

6. Thermal Model of the Disk

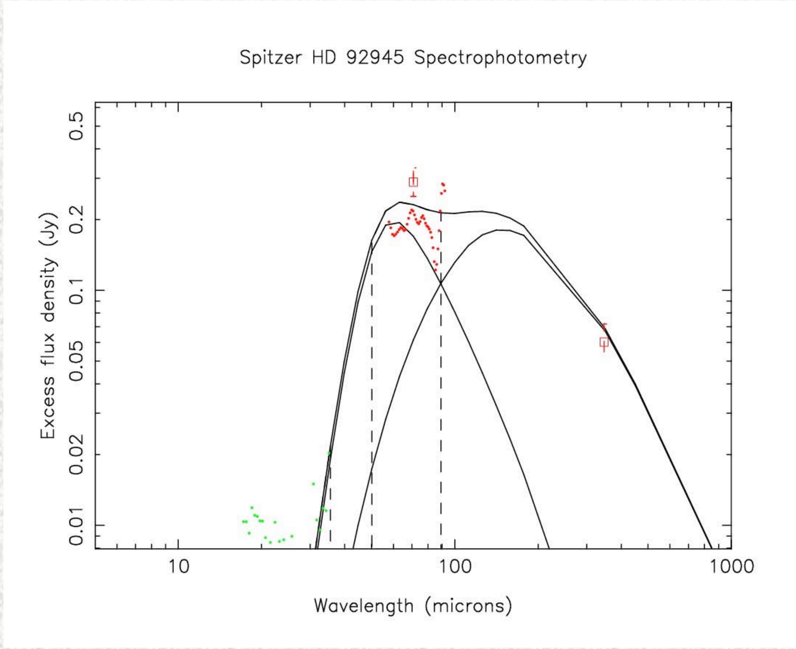

Fig. 7. *Thermal-emission model of the IRS & MIPS spectra and the MIPS & SHARC-II photometry, assuming 2 belts of single-size grains. The outer belt (55–170 AU) consists of 32 μm grains with a surface density profile produced by the scattered-light model in Fig 6. The inner belt (44–55 AU) consists of 14 μm grains with a constant surface density. The need for two components reveals an incompatibility between the Spitzer data at 35–70 μm and the ACS image of the disk within 55 AU (~2″.6).*

7. Summary

❖ We show thermal-IR and optical scattered-light measurements of the debris disk around HD 92945 using MIPS and the ACS coronagraph. This is the 2nd disk around a K dwarf resolved in scattered light.

❖ The disk extends ~45–175 AU from the star, is azimuthally symmetric, and has a bright ring of thickness ~16 AU at r~57 AU. The surface brightness within 110 AU varies as $\sim r^{-1}$ with mean of V~22.5 arcsec^{-2}.

❖ Our scattered-light model shows that the disk is inclined by ~29° and the dust scatters isotropically.

❖ The thermal-IR data can be modeled with a two-component disk divided at 55 AU and having different surface densities and grain sizes (~14 μm and 32 μm).

References:

Chen, C. H., et al. 2005, ApJ, 634, 1372
Kalas, P. et al. 2004, Science, 303, 1990
Kalas, P. et al. 2006, ApJ, 637, L57
Krist, J. E., et al. 2005, AJ, 129, 1008
Silverstone, M.D.2000, PhD Thesis, UCLA